FFI-rapport 2007/02602

Final report: Improvement of the computational methods of the Norwegian Defence Estates Agency for computing noise from the Norwegian defence training ranges

Morten Huseby, Reza Rahimi, Jan Arild Teland
Idar Dyrdal, Haakon Fykse, Bjørn Hugsted, Carl Erik Wasberg

Norwegian Defence Research Establishment (FFI)

Eyvind Aker, Ra Cleave, Finn Løvholt, Christian Madshus, Karin Rothschild

Norwegian Geotechnical Institute (NGI)

Herold Olsen, Svein Å. Storeheier, Gunnar Taraldsen

SINTEF ICT

February 21, 2008

FFI-rapport 2007/02602

1034

ISBN 978-82-464-1322-8

Keywords

skytefelt

støy

vibrasjon

lavfrekvent

måling

Approved by

Jan Ivar Botnan Avdelingssjef/Director

Summary

This report summarizes efforts made to improve the ability of the Norwegian Defence Estates Agency (NODEA) to calculate noise and vibration levels from military activities. Accurate noise maps are essential for conforming to the strict noise emission limits set by the authorities. Failure to do so may ultimately stop or limit the military activity allowed at a training range.

This work has been conducted as a joint 3 year effort with NODEA (FUTURA, FoU) as the client. The project group consisted of FFI, NGI (Norwegian Geotechnical Institute) and SINTEF ICT. During the project period 30 reports, 9 conference proceedings and 1 journal paper have been published.

To estimate the noise level NODEA employs the linear noise propagation program Milstøy (MS), version 2.3.2. Input to MS is a source database for the sound pressure relatively close to the weapon, approximately 250 m for a 155 mm howitzer or 10 m for a rifle. The sound propagation is then calculated to produce noise maps for area planning work by the local authorities. In this project the purpose has been both to enhance the computational methods in MS, and to improve the source database.

During this project we have developed a new research version of Milstøy, version MS 2.4.1 (named NMS). This report describes the new features implemented in NMS (new Milstøy) .

NMS includes new emission data for several weapons, e.g. M109, CV90, 12.7 mm, AG3, C8 and MP7. This improved emission database will greatly improve the noise maps produced for these weapons.

A method has been developed to calculate emission data for a weapon based on geometry, bullet properties and gun powder parameters. This should be helpful when experiments are too expensive or impossible to conduct.

New computational kernels have been developed with special attention to calculate the prediction of low frequency sound, below 100 Hz. The method Nord2000Road is included in NMS. This new version has little in common with the old Nord2000 kernel from MS 2.3.2.

A new low frequency model (LF-model) has been developed to deal with sound below 100 Hz. Motivated by this, the internal structure of NMS has been changed to allow for new types of ground classes. Each new ground class is described by a complex frequency dependent admittance function which varies with air temperature and angle of incidence. These have been computed using the software Multipor, taking into account the acousto-seismic interaction at the air-ground interface.

The new types of ground classes also allow more realistic ground models which are needed for low frequency noise. Further improvements of the calculation of the ground effect have been investigated, and promising novel results have been obtained. These have, however, not been included since the work is not finalized.

An empirical method for propagation of blast noise has been included based on a statistical analysis of measurement data from detonations at Finnskogen. This method also calculates the standard deviation of the prediction.

The NORTRIAL database was developed to facilitate validation of the developed computational kernels. It includes measurements of detonations of C4 at Finnskogen in Norway in 1994 and 1996. NORTRIAL is written in Matlab, and is easy to use for validation purposes. It is freely available on request.

The problem of insulating houses from low frequency noise and vibration has been considered. Unfortunately, no new methods with increased performance for insulating existing homes have been found. However, suggestions have been made about how to build new houses to reduce this problem. New methods for measuring indoor low frequency noise have also been suggested.

Contents

1 Introduction

This report summarizes efforts made to improve the ability of the Norwegian Defence Estates Agency (NODEA) to calculate the noise level from military activity. Accurate noise maps are essential for conforming to the strict noise emission limits set by the authorities. Failure to do so may ultimately stop or limit the military activity allowed at a training field.

This work has been conducted as a joint 3 year effort with NODEA (FUTURA, FoU) as the client. The project group consisted of FFI, Norwegian Geotechnical Institute (NGI) and SINTEF ICT. The continuous contact between NODEA and the joint project has been conducted by Nils Ivar Nilsen at NODEA, FUTURA, Miljørådgivning, luft- og støyforurensing.

To estimate the noise level NODEA employs the linear noise propagation program Milstøy (MS). As input MS takes a source database for the sound pressure relatively close to the weapon, approximately 250 m for a 155 mm howitzer or 10 m for a rifle. The sound propagation is then calculated to produce noise maps for area planning work by the local authorities. In this project the purpose has been both to enhance the computational methods in MS, and to improve the source database.

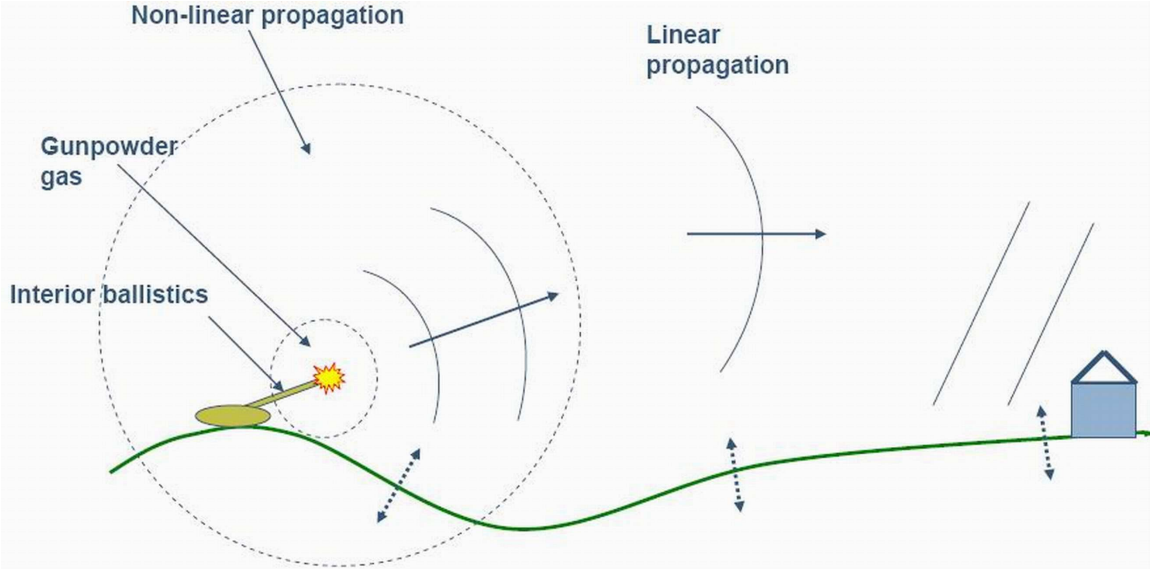

Figure 1.1: The different zones of sound propagation from a weapon.

This report presents an overview the work that has been conducted during this three year joint project. We do not go into detail, but rather mention some main points and provide references to reports and articles that have been published as part of the project (Section 2–4).

Currently NODEA uses MS 2.3.2. During this project we have developed a new research version, MS 2.4.1 (referred to as "New Milstøy" (NMS)). However, since NMS is still a research version, it should not yet be used for production of noise maps of military firing ranges and training fields until

further validation and refinement of the methods have been carried out. Alternatively NMS can be used in parallel with MS 2.3.2 for a trial period.

In Section 5 we show a first test of NMS. Due to limited project resources, it has not been possible to conduct a more comprehensive test, so this must be performed at a later time, before NMS can be set into production.

In this work we have divided the propagation of sound from weapon to receiver into different zones (Figure 1.1). We have considered the interior ballistics when the gun powder burns inside the barrel of a gun, the expanding gun powder gas right outside the muzzle, and the strong non-linear sound close to the weapon. Further away from the weapon we consider the sound propagation to be linear. It is in the start of this linear zone that MS takes its input from the source database. The computation is then performed, by MS, in the linear zone all the way out to the neighbours to the firing range, where measures to reduce noise and vibration inside houses have been considered.

The project work has been divided into three main areas:

1. Emission from weapons
2. Linear sound propagation
3. Insulation of houses from sound and vibration from low frequency noise

2 Emission from weapons

The emission data describe the source strength of the different weapons at the start of the linear zone (Figure 1.1), i.e. 10 m from the weapon for a rifle, and 250 m for a 155 mm howitzer. These data are contained in a database that is used as input to the MS calculations. There is a need to improve and expand this database (more details in Section 2.2). The work with the emission data has been divided into two parts:

1. Analytical/numerical: Development of methods to calculate emission data for a weapon based on information such as geometry, gun powder parameters and the mass of the projectile.
2. Empirical: Measurements and analysis to obtain new emission data for MS.

An overview of some aspects concerning noise from weapons was given in [1]. The report lists some references to literature and ISO and ANSI standards. A couple of known methods are outlined, such as Weber's method [2], as it is applied by Hirsch [3, 4].

2.1 Calculation of emission data

To calculate emission data we employ several numerical codes. The noise emission is modelled through the three zones shown in Figure 1.1. The procedure for estimating emission data for a weapon then consists of the three steps (as suggested in [5]):

1. IBHVG2 calculates the energy emitted from the muzzle. IBHVG2 also calculates the distribution of pressure and particle velocity in the gun powder gas inside the barrel of the gun. This is used as initial condition for AUTODYN.
2. AUTODYN calculates the propagation of the shock wave in the air and in the gun powder gas right after the projectile has left the muzzle. From this calculation we can estimate the directivity of the weapon, i.e. how loud the weapon is in certain directions relative to others.
3. FFIFOFT calculates the non-linear propagation out to the beginning of the linear zone, based on the energy level and the directivity pattern.

2.1.1 Interior ballistics

Burning of the gunpowder and expansion of the gunpowder gas inside the barrel is modelled with IBHVG2 [6]. The end state from this code is then used as initial state for the hydrocode AUTODYN [7] to calculate the shock wave propagation in the zone relatively close to the muzzle. Inputs to IBHVG2 are properties of the gunpowder and the weapon, like chamber volume, length of the barrel and charge weight. Further examples are given in [8]. The code calculates the pressure inside

the barrel and the acceleration of the projectile as a function of time. Of special interest is the state when the projectile leaves the muzzle, as this is used as initial state for AUTODYN simulations.

The most important output variables are mean gas pressure, temperature of the gun chamber, mass fraction of unburned propellant, a summary of energy balance, projectile velocity and breech, mean and base pressures when the projectile leaves the muzzle.

2.1.2 AUTODYN

AUTODYN is an explicit hydrocode for modelling rapid non-linear phenomena. It has been developed by Century Dynamics and is widely used in the weapons effects community. AUTODYN has a number of numerical processors, including Lagrange, Euler and SPH (Smooth Particle Hydrodynamics). It can handle both structured and unstructured meshes, as well as combinations of the various numerical processors in the same problem.

We have used AUTODYN-2D with axial symmetry for the simulations in this project.. This saves considerable simulation time compared with doing full 3D simulations, something which enables us to use a finer grid. However, it is important to be aware that this simplification means that 3D effects are not captured by the simulation. For example, to counter recoil, some weapons have a muzzle brake to redirect propellant gases. This device is usually not axially symmetric, something which has not yet been correctly modelled with the current simulation set-up (as explained in [9]). The correct calculation of the directivity from different types of muzzle brakes still needs more research.

2.1.3 FFIFOFT

For the time being, the AUTODYN-computations have not been performed all the way out to the start of the linear zone, due to limitation in computer resources. Instead the remaining non-linear propagation has been be modelled by other methods. A semi-empirical model called FFIFOFT, which can estimate the non-linear noise level of a weapon is outlined in [10].

The FFIFOFT model is based on the FOFT-model (FOFT: Danish Defence Research Establishment) for spherical explosions [11], where a parametric model is proposed for time series of the sound pressure around a spherical detonation. This model consists of two parts. First, a simple function is fitted to the measured data in [12], to describe the way the peak-pressure and the positive phase duration of a detonation depends on the mass of explosives and the distance from the source. Then, this peak-pressure and positive phase duration are used as input to a formula for the time series of the pressure [13].

In addition FFIFOFT handles directive sources, such as weapons, in a way inspired by [4]. More details are given in [5].

2.1.4 Validation and publication

To verify the results from IBHVG2 and AUTODYN, we have compared with measurements near light weapons [14, 15, 16]. There is good correspondence between calculation and experiment (Figure 2.1). A more comprehensive comparison is given in [9, 10].

The results from this work have been presented at two conferences [17, 18] and also published in the Noise Control Engineering Journal [9]. Figure 2.1 shows a comparison of measured and calculated sound pressure 80 cm from the muzzle of the AG3 (7.62 mm) rifle, without recoil break.

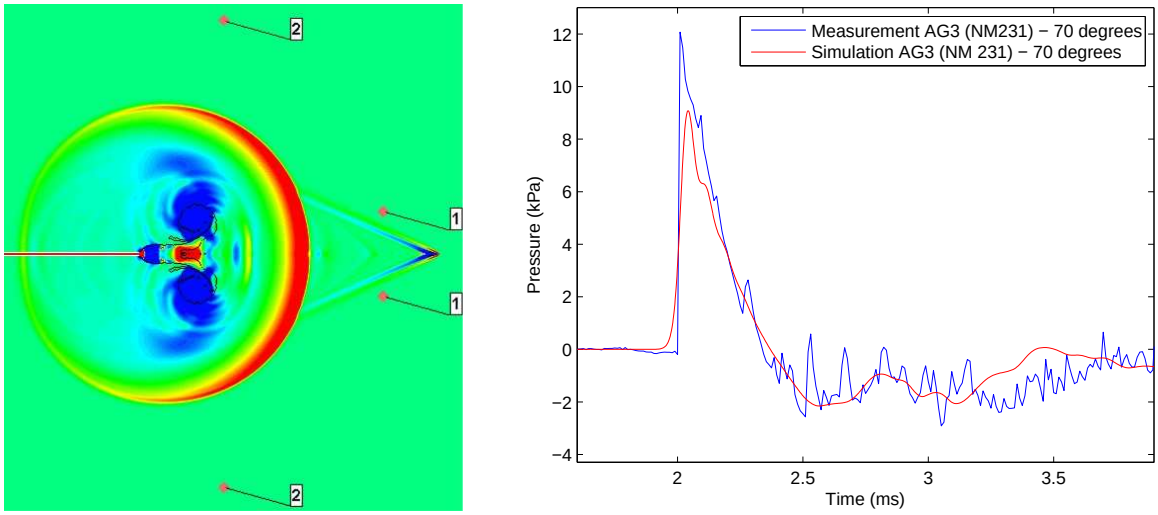

Figure 2.1: Calculation with IBHVG2 and AUTODYN for AG3 (7.62 mm rifle) without recoil dampener. Left side: Pressure field. Right side: Time series of the pressure, measurement and calculation.

2.2 Measurement of emission data

Emission databases containing the source strength of different weapons at the start of the linear zone are expensive and time-consuming to develop. As a result of this, such databases are often old and seem to have limited documentation on both the measurement conditions and the specific type of weapon measured. For example the emission data for a 155 mm weapon may not state specifically the type of weapon, even though the noise level from a M109 field howitzer may be considerably different from e.g. the Archer artillery gun which has a considerably longer barrel and a different muzzle break. Also parameters like amount of propellant charge and angle of elevation are rarely mentioned in the documentation.

New weapons that are taken into use by the Norwegian Defence, need to be added to the database. Such databases are not very well suited for exchange between countries, due to the fact that most countries have different weapons with special modifications.

To improve the situation, FB has expressed a desire for emission data of new weapons to be obtained and included in the database together with updates to source data for existing weapons. Several campaigns of measurements have been conducted during the project, both to find emission data, and to validate our computations close to the weapon.

As part of this work, several Matlab programs were developed, to calculate the emission data. A joint effort was made to verify the programs for calculation of 1/3-octave spectra for sound exposure level [15, 19]. A Matlab routine for the calculation of these spectra is provided as part of the NORTRIAL database (Section 3.4).

In [15, 20] we describe the calculation of emission data, including semi-automatic detection and isolation of muzzle blast (typically 70 to 200 time series for each weapon), removal of the ground effect, energy mean over several shots, and directional interpolation/extrapolation.

2.2.1 Small calibre weapons

In Dompa (measurement site at FFI) we measured the sound pressure at 80 cm from the AG3 (7.62 mm) and C8 (5.56 mm) rifles [14]. This was done in two directions (10 and 70 degrees), to validate calculations.

At Terningmoen in 2005 we performed measurements both at 80 cm and at 10 m from the weapon, with assistance from FLO T&V (Norwegian Defence logistics organization, test and verification). We measured 14 weapons, among them several weapons currently in use in the Norwegian defence, without any available emission data. The weapons measured were: AG3 (NM60), AG3 (NM231), C8, Steyr AUG, G36, G36C, P90, Glock P80, MP5, MP7, Sauer, MG3 and FN MAG (two barrels). To be able to remove the effect of the ground reflection, the type of ground at the test site was measured and documented in [21]. The documentation of the measurements and emission data for MS is given in [15].

Figure 2.2: Emission measurements of small calibre weapons at Terningmoen.

2.2.2 CV90 (30 mm) and NM218 (12.7 mm)

At Rena in 2006 we conducted measurements of CV90 (30 mm), NM218 (12.7 mm machine gun) and 40 mm AGL (automatic grenade launcher). Data were collected both near (2 m) and further (20 m) from the weapon. Documentation of the measurements is given in [16]. The data were analyzed and emission data for MS was given in [22]. The muzzle noise from the AGL was found to be so low that it does not need to be included in calculation of noise maps.

Figure 2.3: Emission measurements of 30 mm and 12.7 mm at Rena.

2.2.3 M109, 155 mm

At Hjerkinn in 2006 FFI and NODEA performed measurements of the M109 155 mm field howitzer (Figure 2.4). The measurements were made at Turrhaugen, in 7 directions in a semi-circle at 250 m from the weapon. We also performed measurements close to the weapon (20 m) to validate our computations with IBHVG2 and AUTODYN. The M109 is one of the noisiest weapons of the Norwegian Defence, and therefore sets limitations on planning and running of firing ranges. The M109 was loaded with maximum charge (5 modules DM72) during the measurements. The measurement campaign is documented in [23]. The data is analyzed and emission data for MS is produced in [20].

2.3 Near field acousto-seismic response

As a part of the M109 test program discussed in subsection 2.2.3 the response of the air and soil in the near field was measured. Sound pressure was recorded above, at, and below ground level, and vibration was measured at and below ground level (Figure 2.5). A study of the data has been performed, details of which can be found in [24].

Figure 2.4: Emission measurements of M109, 155 mm field howitzer at Hjerkinn.

Figure 2.5: Near field measurement setup.

3 Linear sound propagation

There has been a wish to improve the linear propagation kernels in MS. During the project, several new methods have been introduced.

The kernel currently used by NODEA for making noise maps is the Industry Noise model [25]. In addition an early version of the Nord2000 method is available [26, 27]. In NMS the new and improved Nord2000Road is included, containing the point to point procedure COMPRO16 [28]. NORD2000Road has been developed in a larger Nordic cooperation on noise from roads.

None of the kernels mentioned above are capable of handling low frequency noise (below 25–100 Hz). As an example it can be noted that Nord2000Road calculates formally down to 25Hz, but the accuracy of the calculations below 100-200 Hz can not be trusted. The model is originally developed and fine tuned with particular focus on road vehicle noise, and the main source is then around 1kHz and the propagation distance is typically < 1km.

To improve on this situation a new low frequency model (LF-model) has been developed (Section 3.2). This model is very simplified, not containing topography and meteorology, but should still capture effects not previously included in MS. The LF-model applies a complex admittance which in addition to being dependent on frequency also depends on temperature and angle of incidence (Section 3.3). These admittance values are precalculated for different ground types, angles and temperatures. A new structure has been implemented in NMS in order to include the new variations in the precalculated admittance [28].

To facilitate validation of these new models the database NORTRIAL (Section 3.4) was used. NORTRIAL contains a comprehensive set of measurements of C4 detonations in Norwegian forest terrain. Some tests of NMS are presented in Section 3.8 and Section 5.

Using data from the NORTRIAL database a statistical analysis was made to arrive at an empirical model for the sound exposure level (Section 3.5). This model is implemented in NMS. There are three choices for this kernel: Expected SEL, expected SEL minus standard deviation and expected SEL plus standard deviation.

3.1 New functionality in MS

Implementation of the above mentioned computational kernels has led to slight modification of the user interface of NMS. These changes are described in [28].

3.2 LF-model

Here we describe the LF-model included in NMS. A more detailed description together with definitions of variables and parameters are given in [29].

3.2.1 Simple physically based ground models

One reason for the success of the Delany-Bazley [30] ground impedance model is that it depends on only one parameter σ_e for each frequency f. It is, however, well known that it fails at low frequencies, and the corresponding time-domain model is awkward. The possibly simplest alternative without these effects is given by the model [31][32, p.73]

$$\beta_n = \sqrt{\frac{7}{5}}\Omega_e \left(1 + \frac{i\Omega_e\sigma_e}{2\pi\rho_a f}\right)^{-\frac{1}{2}} \tag{3.1}$$

The quantity β is the specific normalized admittance of the air-ground interface. The value $\rho_a = 1.1899\,\mathrm{kg\ m^{-3}}$ corresponding to air at $20\,℃$ [33, p.29-30] will be used here.

This model is made into a one-parameter model by the following relationship between effective porosity Ω_e and effective flow resistivity σ_e

$$10\lg(100\Omega_e) = \frac{1}{2B}\left[\, -y + A + 20B - \sqrt{4BC + (-y + A - 20B)^2}\,\right] \tag{3.2}$$

where $y = 10\lg(\sigma_e/\sigma_0)$, $\sigma_0 = 1\mathrm{kNsm}^{-4}$, $A = 206.95$, $B = 9.88$ and $C = 13.82$.

The form is as simple as possible, but chosen so that the asymptotic behaviour at $\Omega_e = 1$ and $\Omega_e = 0$ are physically reasonable. The particular numerical values for the coefficients A, B and C have been determined by comparison with the Delany-Bazley model.

Let

$$\beta = -i\beta_n f_\theta \tan g_L \tag{3.3}$$

with $f_\theta = \sqrt{1 - (\beta_n/\Omega)^2 \sin^2\theta}$, and $g_L = f_\theta L\Omega 2\pi f/(c\beta_n)$. This gives a simple 3 parameter model for a hard-backed layer of thickness L and porosity Ω. The parameters are given by an effective thickness $L\Omega c_0/c$, the porosity Ω, and the effective flow resistivity as above. The sound speed in air is c, and $c_0 = 344$ m/s is a reference sound speed.

The dependence on the angle of incidence θ is typically weak, and $f_\theta \approx 1$ is then a good approximation. The result is then a simple two-parameter model, which depends on the effective flow resistivity and the effective thickness of the layer.

It must, however, be observed that small changes in β can result in rather large changes in the ground effect in certain cases.

3.2.2 The boundary loss

The pressure field p from a point source above a plane is given by

$$p = e^{ikR_1}/R_1 + \mathcal{Q}e^{ikR_2}/R_2. \tag{3.4}$$

This defines the spherical wave reflection coefficient $\mathcal{Q}$.

The equation

$$\mathcal{Q} = \mathcal{R} + (1 - \mathcal{R})\mathrm{F} \tag{3.5}$$

defines the boundary loss F. The plane wave reflection coefficient $\mathcal{R}$ and the wave number k are given in addition to p.

The geometry is determined by the cosine of the angle of incidence $\delta = \cos\theta$ and the distances R_1 and R_2 from the source and mirror source, respectively.

The grazing incidence case $\delta = 0$ gives $\mathcal{R} = -1$ and

$$p = 2Fe^{ikR_1}/R_1. \tag{3.6}$$

This equation motivates the use of the term "boundary loss".

The Sommerfeld approximation is given by

$$F \approx F_S = 1 + i\sqrt{\pi}\rho^{\frac{1}{2}}w(\rho^{\frac{1}{2}}), \tag{3.7}$$

where ρ is the numerical distance and

$$\rho^{\frac{1}{2}} = \frac{1+i}{2}\sqrt{kR_2}\frac{\beta+\delta}{\sqrt{1+\beta\delta}}. \tag{3.8}$$

The $\sqrt{\cdot}$ denotes the principal value of the square-root, and β is the specific normalized admittance of the plane.

The Fadeeva error function [34, formula (7.1.8)]

$$w(z) = e^{-z^2}(1 + \frac{2i}{\sqrt{\pi}}\int_0^z e^{t^2}\,dt) = \sum_{n=0}^{\infty}\frac{(iz)^n}{\Gamma(1+n/2)} \tag{3.9}$$

is an entire function, and the square-root $\rho^{1/2}$ is the only source of difficulties in equation (3.7). The correct square-root of the numerical distance ρ is given above.

Sommerfeld, and his successors, derived the expression for F_S under the assumption $|k|\,R_2 \gg 1$. He observed further that the case $|k|\,R_2 \gg 1$ and $|\rho| \ll 1$ is important in applications.

It is, however, well known empirically that the formula for F_S remains valid in certain cases even without the requirement $|k|\,R_2 \gg 1$. This has been discussed by Taraldsen [35, 36].

In the case of a locally-reacting ground, it has been shown that the exact boundary loss depends on two dimensionless distances ρ and τ [37]. The above version of the Sommerfeld approximation follows simply by deletion of the term containing the second numerical distance τ.

The Sommerfeld approximation can also in certain cases be taken as an approximation in the non-locally reacting case, with admittance given at the angle of incidence. This is consistent with the original Sommerfeld approximation, and has also been verified for certain layered models [38, 39, 40, 41, 42, 32]. This has been implemented in NMS.

A final warning: Note that there is only one surface wave component included in the Sommerfeld approximation. This is in contrast to the above-mentioned possibility of many different kinds of surface waves.

3.2.3 One example

Figure 3.1 gives the ground effect in a case with a snow layer. The model for the ground is given by equation (3.3). The parameters have in this case been chosen with some care to demonstrate a particular phenomenon: At a certain distance (150 m) and for a certain frequency the sound disappears, but comes back further away. This is similar to the well known phenomena of shadow zones due to special meteorological conditions, but in this case the effect is due to the snow layer. The peculiarity of the phenomenon is that it can not be explained as interference between the direct and the reflected wave: The phenomenon persists in the case where the source and receiver is at the ground and the wave is a surface wave travelling along the surface.

Figure 3.1 is the result of numeric integration of the Sommerfeld integrals, and the computational cost was 22 hours. A corresponding figure with the method implemented in Milstøy takes 90 seconds. This particular case gives also an example where the implementation gives results which deviates from the exact, and motivates the inclusion of new improvements.

3.2.4 Final comments

It is recommended to continue the study of the ground effect in the particular case of low frequencies. The Sommerfeld approximation, which is used here, can give large errors in the prediction even in the case of a locally reacting ground. This is even truer if more realistic ground models are used.

A completely satisfactory theory in the case of a locally reacting ground is within reach, but it has not been possible within the completion of this project. A detailed study of the non-locally reacting case is feasible, but the amount of work here could correspond to more than one PhD degree.

Prediction of sound without proper modelling of the ground effect will certainly give errors of the order of 5 dB. Furthermore, special cases with errors of the order of 10 dB or more should come as no surprise.

3.3 Ground classification

The propagation of low frequency sound is affected by meteorological properties such as temperature and wind strength, as well as by the ground cover and geology. Therefore, for an accurate prediction of the levels of sound and vibration at a certain location, the ground cover and geology along the propagation path must be accounted for.

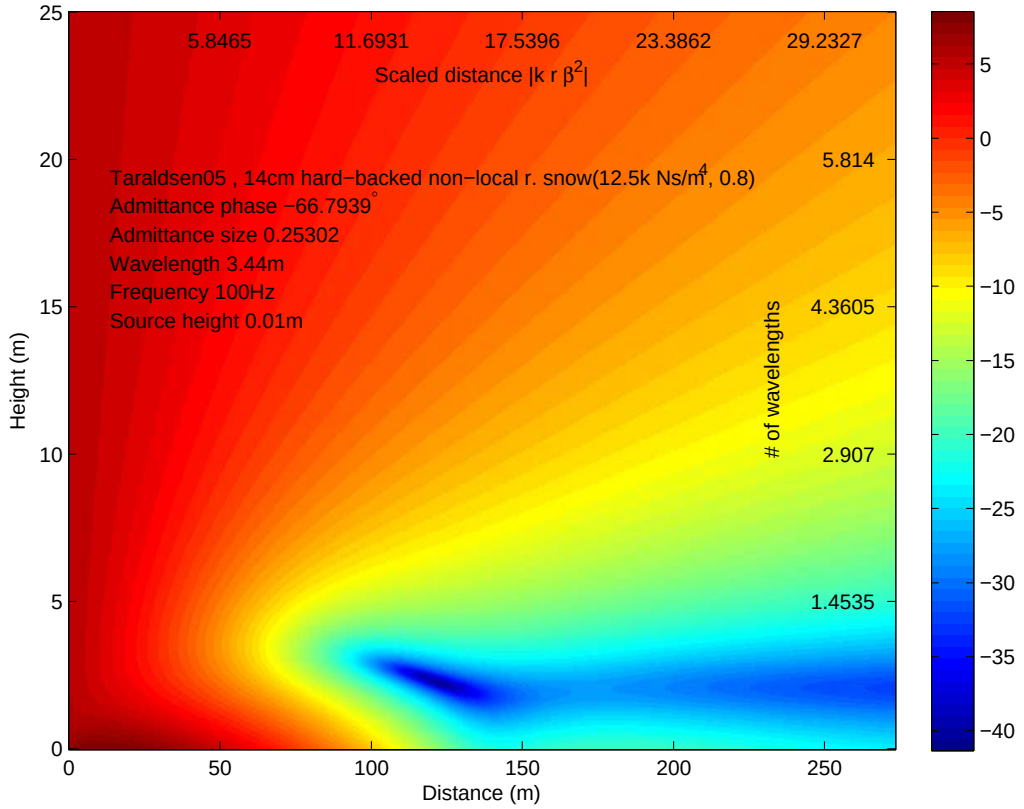

Figure 3.1: Ground effect over snow.

A new method of ground classification has been developed for NMS. It builds upon the system used in MS, which consists of 7 ground cover classes, by incorporating the effects of underlying geological layers. Furthermore, in contrast to the previous ground classes, the new classes take into account the complex layering inherent in soil and rock, and the acousto-seismic interaction of the air and ground waves, in addition to the rigid frame porous interaction that was taken into account in MS.

The ground classification makes use of the current MS ground classes A-G, as these have existed in both MS and the Nord2000 prediction model for many years. In the new ground classes, the ground classes A-G are interpreted as surface classes or main classes. For each surface class, there are up to 7 sub-classes determined by the sub-layers. Vegetation maps are used to first classify the predominant surface class over the propagation path, and geological maps are then used to categorize the underlying ground type. All geologically possible combinations of surface and subsurface form the new ground classes (see Table 3.1). A total of 31 different ground classes are therefore available in the new Milstøy (NMS).

Each ground class is described by a complex frequency dependent admittance function which varies

		Snow	Soft ground	Marsh/peat	Forest/cultivated/ inhabited area	Activity area/gravel road/parking lot	Hard surface (rock, glacier, etc)	Water
		A	B	C	D	E	F	G
Homogeneous	0		x				x	x
Rock	1	x		x	x	x		
Clay and silt, soft	2	x		x	x	x		
Clay and silt, moderate	3	x		x	x	x		
Loose sand	4	x		x	x	x		
Normally compacted sand	5	x		x	x	x		
Moraine	6	x		x	x	x		
Loose gravel and rock	7	x		x	x	x		

Table 3.1: New ground classes, showing the chosen combinations of ground covers A-G with the underlying sub-layers 0-7.

with air temperature and angle of incidence. The admittance functions for each of the ground classes given in Table 3.1 have been computed using the software Multipor, which was developed as part of previous R&D projects on sound and vibration. It has been extensively verified against more traditional impedance solvers as well as experimentally verified against the Finnskogen 3.06 site (see [43], Appendix A). The main motivation for using Multipor was its capability of including layered media and the acousto-seismic interaction, which are usually not taken into account. The admittance functions have been calculated for each 1/3-octave frequency band from 1 to 100 Hz, for temperatures ranging from -30 to 30 C, and for angles of incidence between 0 and 90 degrees. The temperature resolution is 5^oC, and the angle of incidence resolution varies from 1 to 5 degrees (1 degree near grazing angles of incidence).

The main influence of the new ground classes and their impedance functions occurs at low frequencies: the magnitude of the impedance functions varies only slightly for the various classes, however, the phase changes considerably. These phase effects can strongly affect the low frequency attenuation over the propagation distance, e.g. for the LF-model described in Section 3.2.

Further details regarding the new ground classes and calculation of impedance functions are given in [43].

3.4 NORTRIAL database

The NORTRIAL database was developed to facilitate validation of the developed computational kernels. The database and supporting functions have been used in this research project to provide datasets for the development of empirical models of sound and vibration propagation (subsection 3.5), and to validate results from analytical low frequency sound propagation models (section 5).

NORTRIAL gathers sound and vibration measurements from military activity in Norway. It includes raw and processed sound and vibration data as well as meta data such as weather conditions and ground cover. The database has both summer and winter measurements, and the data covers propagation distances varying from 110 metres to 15 kilometres.

NORTRIAL is implemented in the Matlab environment, and comes with supporting functions to aid in data extraction, manipulation and processing. Users can expand this functionality with their own routines. Figure 3.2 gives an overview of the structure of a data element, while more detailed descriptions of the NORTRIAL data structure and supporting functions are given in [44] and [45].

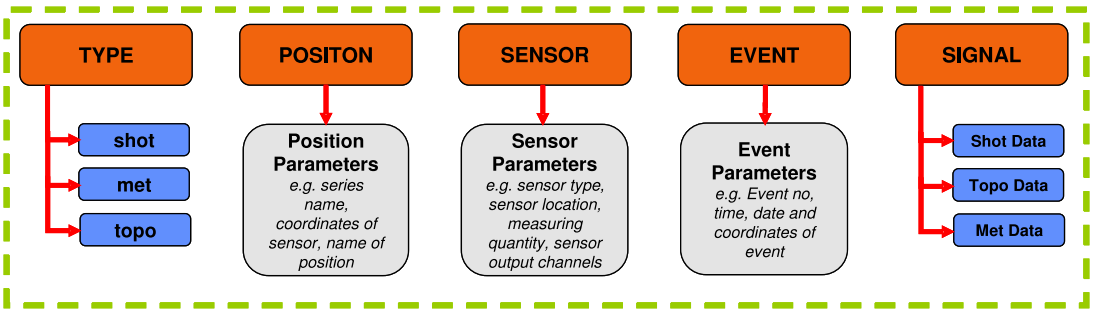

Figure 3.2: The structure of a single NORTRIAL data element.

As of writing, NORTRIAL comprises data from the Lista tests of 1992 [46], the Finnskogen tests of 1994 and 1996 [47, 48], the Haslemoen tests of 1994 and 1995 [49], and the Rødsmoen tests of 2005 [46]. These tests are summarized in Table 3.2. NORTRIAL will be updated with new data as new test series are performed.

The existence of NORTRIAL and its public availability was announced at [50]. The database can be obtained by contacting NGI (see http://nortrial.ngi.no).

3.5 Empirical modelling

For source to receiver propagation distances of several kilometres, sound measurements can display an apparently random variability of several tens of dB. Although some of this variability could be explained using more sophisticated modelling tools, ones that better account for parameters such

Test series	Year	Season	Charge	# shots
Lista	1992	Winter	Dynamite	12
Finnskogen	1994	Summer	C4	167
Finnskogen	1996	Winter	C4	240
Haslemoen	1994	Summer	C4	29
Haslemoen	1995	Winter	C4	88
Rødsmoen	2005	Winter	C4	59

Table 3.2: Overview of NORTRIAL test data.

as wind, temperature, terrain and ground interaction, there will still remain a substantial variability that is either purely stochastic or caused by other factors outside our knowledge and/or control.

MS lacks an empirical model of the sound propagation. During the project, two such models have been developed, both of which are based upon the Finnskogen data series mentioned in subsection 3.4. An empirical relationship gives the expected Sound Exposure Level, as well as the expected stochastic variability of this exposure. This has been implemented in NMS.

3.5.1 Statistical analyses

Using the 1994 Finnskogen data from the NORTRIAL database, and applying various statistical techniques, an initial empirical sound propagation model was developed. The Sound Exposure Level, L_E, was chosen as the response variable for the model, and a qualitative data assessment of L_E for the 1994 Finnskogen data resulted in a reduced data set of 561 observations. The 28 explanatory variables that were measured were prioritised using partial least squares regression and principle component analysis. Based on these analyses a preliminary model with a reduced number of explanatory variables was established [51]. These variables include the source-receiver distance in metres, R, the charge mass in kilograms, Q, the cosine of the wind direction, $\cos(\theta)$[1], and the percentage of forest cover, T.

Based on the work described above, the preliminary empirical model was improved by adding both the receiver height and weather parameters to the explanatory variables and considering L_E as well as the 1/3-octave spectrum of L_E as response variables. The meteorological effect is a parameterisation of a combination of the temperature and wind profiles. The regression parameters A, B, and C provide a log-linear directional sound speed propagation profile. For the improved empirical model, a total of 2187 sound recordings were used. In addition to the linear regression model, both a non-linear multiple regression model as well as a Bayesian method were used in generating alternative models for verification of the model assumptions.

Based on the linear multiple least squares method, the following frequency independent model was

[1] θ is relative to the source-to-receiver distance.

established:

$$L_E = 120.69 - 27.10 \log_{10}\left(\frac{R}{Q^{0.399}}\right) - 0.08F + 0.01H + 1.25A + 199.69B + 0.20C. \quad (3.10)$$

Similar coefficients were obtained using the non-linear least squares and the Bayesian methods, showing that the more simple linear multiple least squares are behaves well.

The frequency dependent model reads:

$$L_E = L_0 - b_1 \log_{10}\left(\frac{R}{Q^{-b_2/b_1}}\right) + b_3 F + b_5 A + b_6 B \pm \epsilon, \quad (3.11)$$

where,

$$L_0 = b_0 + H b_4 + C b_7. \quad (3.12)$$

L_0 is a modified reference spectrum, and results from the strong correlation between the term b_0 and b_4 and b_7. Because of this strong correlation, it is considered to be a better reference spectrum reference than b_0. In the frequency dependent model each of the regression coefficients b_0—b_7 vary with frequency. The exponent $-b_2/b_1$ approaches unity at low frequencies and zero at the highest frequencies.

The implementation of the empirical model in NMS uses tabulated values for the regression coefficients b_0—b_7 and the error ϵ. These tables may be found in [52], Appendix A.

3.6 Consideration of new linear models

As mentioned above, MS contains several computational kernels. During the project work we considered the feasibility of constructing new or including existing cores that was distinctively different from the existing ones. No cores were found that could be implemented with the resources allocated for this subtask. However, for completeness, in this subsection we mention two of the models that were considered. The code FEMNOISE was considered for a reference model. The ray-tracer XRAY was considered as a possible core for MS.

3.6.1 FEMNOISE

The computational cores in MS are fast methods, where several simplifications have been made. To evaluate the effect of such simplifications, it is desired to have a computational reference model. A reference model may use more computational resources, because it is not meant to be implemented in MS. Instead it can provide reference solutions of greater accuracy.

One such effort was the finite element code FEMNOISE. The model was implemented as a 3D finite element method in space and an explicit finite difference scheme in time. The model was first formulated in [53] as a 3D rigid frame Biot model [54]. Here the fluid flow is solved both in the air and in the porous ground, allowing the ground to be non-locally reacting. In [55] focus

was on running and validating the code in 3D on real life data over an actual terrain profile from Finnskogen in Norway. The code was running on the parallel computer at FFI. In [56] FEMNOISE reached its final formulation, now based on the equivalent fluid model following Fellah [57, 58]. This lead to quite similar equations as the Biot formulation. Finally, in [5] emphasis was on methods implementing a realistic weapon source into the code.

The main problem with FEMNOISE is the high demands on computational resources. Its strength is that it can include complex 3D geometry 3.3). Such geometries are however not often encountered and computational speed is then more important.

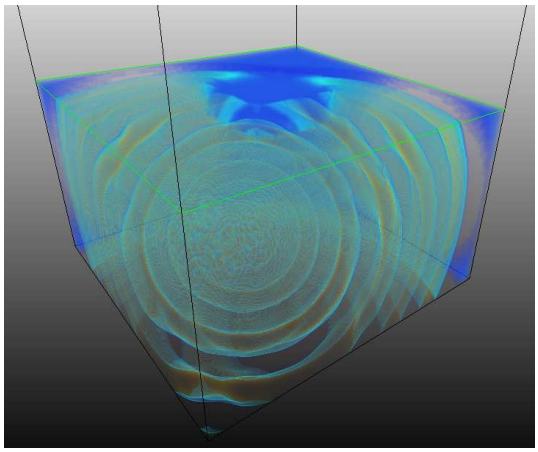

Figure 3.3: Three-dimensional propagation of sound from a harmonic source in air propagating into and around a box of porous ground. Isosurfaces of the pressure field are visualized.

3.6.2 XRAY

With its broad experience, e.g. from underwater acoustics, the Swedish Defence Research Agency (FOI) have made a ray-tracer called XRAY, for calculating the noise level from weapons. In a joint work with FFI, this code was tested against measurements from the NORTRIAL database [59]. Taken into consideration the very demanding data set that was chosen, the results were regarded as promising. However, it seemed that XRAY was not mature enough to be considered for inclusion into NMS, given the time constraints of the project.

XRAY was tested at Swedish firing ranges in 2007, with good feedback from the users [60]. XRAY is no longer being developed for use at firing ranges. The development of XRAY is now (in 2008) being done for noise from windmills.

3.7 Scaling of prediction levels for height above sea level

A scaling of emission data to account for height above sea level was given in a simple formula in [61], Appendix A. This scaling takes into consideration that at higher altitudes and lower temperatures the sound levels will be lower and the length of a pressure pulse will be longer. This scaling is not implemented in NMS. The correction to L_{CE} due to this scaling is in most cases less than 1 dB (often less than 0.5 dB).

3.8 Preliminary testing of NMS

During the work with NMS, some work was done in parallel to test the iterative improvements. These tests were conducted with a modified version of MS 2.3.2. To facilitate such tests, a selection of measurement data (C1) was made from the NORTRIAL database (Section 3.4). This selection contains data from detonations of C4 explosives measured at Finnskogen in Norway in the summer of 1994, for distances from 2 to 16 km. The data selection was collected in the report [62], which also serves as a first example of how to employ the NORTRIAL database.

In [63] MS was tested on the data selection C1. The test case is very demanding, being hilly and over varying ground types. For this test case the calculations made with MS 2.3.2 showed poor comparison with the measurement data.

In [61] a similar test was conducted on data from Haslemoen (C2), also available in the NORTRIAL database. Here the test case was less demanding, and good agreement was found between MS 2.3.2 and the measurements.

4 Insulation of houses from sound and vibration from low frequency noise

Close to some military installations the noise level can not be controlled, with the consequence that some neighbours experience an unacceptable noise level (Figure 4.1). One way to avoid this is to reduce the indoor noise level by insulating the house. One task in this project the task was to specify methods (if any) to better insulate building against low frequency sound and vibration.

Initially a literature study was performed. At Rødsmoen measurements was done to investigate the attenuation of outdoor low frequency impulse noise in a house (Section 4.1.1).

A system for unattended measurements of sound and vibration has been set up at Rødsmoen [64], intended as a measurement facility for low-frequency sound and vibration time series recordings. Preliminary recommendations for the management and use of this facility was formulated in [65].

It has not been possible in the present project to identify new measures that can be taken to improve insulation of existing houses from low frequency noise. However some suggestions are made about construction of new houses in areas where noise is believed to be a problem (Section 4.1.2).

It is also pointed out that better methods are needed for measurements of indoor low frequency noise (Section 4.2). Without such methods the effect of insulation measures can not be assessed.

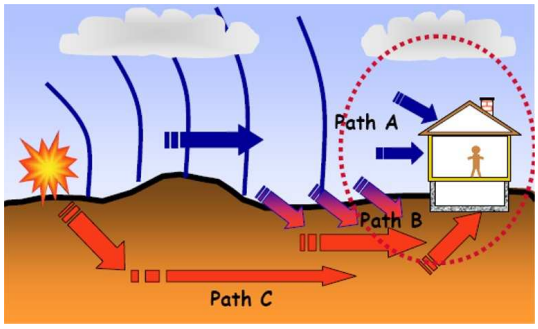

Figure 4.1: Three possible propagation paths from a LF-source to a building.

4.1 Building insulation - Rødsmoen tests

Previously performed studies have shown that for low frequencies, building vibration rather than the audible sound is often the major cause of annoyance. The insulation of the building, as well as the physical mechanisms governing the transfer of energy from external sound to internal sound and vibration were of primary interest for the study described in this section. Without such understanding it is not possible to develop efficient sound and vibration insulation for low frequencies.

4.1.1 Rødsmoen tests

The Rødsmoen data mentioned in section 3.4 were acquired as a part of this research programme. There were four measurement sites, whereof two comprised outdoor sound measurements, and two comprised indoor and outdoor sound and vibration measurements. The "SIBO" building, one of the sound and vibration sites, was instrumented with the aim of investigating the effect of low frequency sound on a typical one storey Norwegian wooden dwelling (Figure 4.2). A similar but

Figure 4.2: Instrumentation inside the SIBO building.

less comprehensive instrumentation was performed in the second sound and vibration measurement site (subsequently labelled the "B1" house).

Processing of these data is being done in a related project. The instrumentation can be summarised as follows:

- → Ground vibration outside the house, arranged in a triangular array in order to assess the direction of vibration propagation
- → Free field sound pressure outside the building
- → Sound pressure on the outside of building roof
- → Floor vibration of the cellar level and first floor
- → Wall and window vibration
- → Sound pressure inside the building

The acoustic source was C4 of 1, 5 and 15 kg, and approximately 60 explosions were recorded (about 1.6 km and 0.9 km from the SIBO and B1 buildings respectively).

4.1.2 Analysis of building insulation

The analysis of the data has been done under a related project which concentrates on the building insulation, and is summarised in detail in [66].

The main findings for the "SIBO" house revealed fundamental knowledge about the dynamic performance of this type of building when exposed to transient sound pressure with respect to low frequency sound and vibration insulation. These findings are summarised below.

- → Making the total rigidity and first natural frequency of the whole building as high as possible will efficiently reduce the transfer of outside sound pressure into the building.
- → To reduce sound transfer also at the natural frequency and above, increased damping is beneficial. Added mass should be used with care.
- → Large window areas should be avoided.
- → Damping may be obtained by non-symmetrical forms and uneven length of major load-carrying members.
- → Structural solutions which reduce the rotational rigidity between walls and floor may effectively reduce floor vibration.
- → To reduce acoustically driven floor vibration, floors should be as rigid as possible and have high natural frequencies. Added floor damping can be obtained by arbitrarily changing the span between support points for the floor beams.

The measured vibration insulation from "SIBO" and "B1" were surprisingly consistent with two other measurements at Asprusta and Gildeskålveien in Bodø. However, the "SIBO" house revealed clearly better insulation properties with respect to floor vibration in the low frequency range than the other buildings investigated. However, we stress that still only a few buildings have been analysed with respect to low frequency sound and vibration insulation. Moreover, additional measurements in other buildings, with more elaborate instrumentation, is required to better understand the generation mechanisms and variation of low frequency vibration in the various kinds of typical Norwegian residential buildings. This is also valuable to avoid excessive sound and vibration exposure to military personnel close to explosive sources.

4.2 Measures against low frequency sound and vibration impact on buildings

Low frequency sound and vibration insulation in buildings is a complex issue. The phenomena that governs the insulation properties are only partly known. Theoretical models are almost non-existing, and knowledge about practical methods for sound insulation at very low frequencies are of a meagre and unsatisfactory kind. Existing building codes and regulations seldom address sound components below about 50 Hz, even though noise and vibration at lower frequencies can cause

considerable annoyance. NODEA has initiated a pilot study to address problems concerning low frequency sound insulation in buildings. This study has been a cooperation between the following research institutions: Chalmers, NTNU, NGI, and SINTEF, and sums up the results from a workshop and several meetings held in connection with the pilot study [67].

(The remaining part of this subsection consists of the conclusion in [68].)

Techniques for achieving good sound insulation are well known for frequencies above 100 Hz. Theoretical models for calculating the sound insulation at these frequencies also exist.

There are some data and results from practical experiments for sound insulation in the frequency range 50 - 100 Hz, but below 50 Hz very little systematic knowledge is available.

Models for calculation of the insulating properties of building constructions at low frequencies are also almost non-existing. Some models and literature are presented in the thesis by Pietrzyk [69].

Nordic building traditions call for light constructions. There is thus a great demand to find constructions that have sufficient mass or stiffness to control the resonances at low frequencies. Dynamic response properties of typical Norwegian single- or multiple family buildings are generally not well known, and particularly not how these properties develop over the life-time of the building.

There is an urgent need to develop new methods for building acoustic measurements at low frequencies. The challenge is two-fold. The methods must yield sufficiently accurate results in the sense that the results can be readily reproduced by repeated measurements. It is also vital that the results, i.e. the parameters that are being measured, are relevant for the intended purpose.

Measurement of LFN (Low Frequency Noise) insulation, for instance, must really reflect the way the insulating properties are subjectively perceived. Measurement methods that can quantify rattling in a representative way and how it relates to the LFN and building vibration are also in urgent need.

The availability of relevant measurement data is not satisfactory. This stands in contrast to the large number of buildings close to for instance airports or major roads where sound insulation has been performed. It is strongly suggested that before and after sound insulation measurements are performed and systemized in future projects. These measurements must come in addition to measurements that cover the middle and high frequency range.

The case studies presented here demonstrate the urgent need for a measurement standard with focus on LFN annoyance.

It is suggested to use a variant of the method proposed by Pedersen et al. [70] to measure the indoor LFN level. The simplest version is given by at least one external microphone and 4 corner microphones inside a room. The room can for instance be selected on the basis of the experience given by the persons living in the building, and the 4 corner positions can possibly be chosen as the 4 ceiling corners. If the noise source consists of series of events, the extreme case being a series of explosions, then a sufficient number of events must be logged and measured. This must be

done before and after the sound insulation. The work by Pedersen et al. [70] strongly suggests that this will lead to a simple, repeatable and well defined measurement of the effect of the LF sound insulation.

This should be complemented with at least one floor vibration measurement, and if possible the vibration of the most exposed window.

A summary of the suggestions is given by:

1. Do measurement for the actual sources occurring
2. Measure before and after the sound insulation
3. Use a measurement method that is well adapted to low frequency noise
4. Do not forget the middle and high frequency range

Recent findings [71] indicate that the unweighted sound exposure level L_{E}, or possibly the L_{CE}, should be used in the measurements if a single number level is needed.

5 Test of new Milstøy

Here we present some early tests of NMS. The evaluation of different prediction methods in NMS is based on comparing the predicted values with some available sound measurements. We arranged two different cases from the measurements in the NORTRIAL database (C1 and C2). In addition we compare with measurements from the M109 155 mm howitzer at 7 km. For a detailed description of the cases see [62, 63, 61, 23, 20].

The measurements at 7 km are a very relevant example of noise levels at the limit of what is permitted. The measurements were done at a neighbour 7 km from the firing positions. The C-weighted sound levels were very close to 100 dB, which is a maximum level for large weapons. During this measurement campaign emission data were also produced [20]. This strengthens the accuracy of the comparison.

MS as a sound prediction tool is under continuous development. Our testing is done with NMS, which includes all different prediction methods available in this project. The Nord2000Road (N2R) is a new (very different) version of the Nord2000 method and is implemented in NMS. N2R includes the point to point calculation routine COMPRO16.

The new method for ground classification that has been included in NSM (Section 3.3) could not be applied in these tests. At the present time these methods have only been tested at artificial maps constructed for verification during the implementation of the new parameter structure. To test this feature NODEA will first have to acquire the maps needed.

The results from testing MS on C1 and C2 are summarized in tables 5.1 and 5.2. Table 5.1 is for the summer 1994 in NORTRIALS. The file number is the specific event number in the database. Dist is the distance between the source and receiver, the value in the C4 column is the charge weight, and the measurement column is the $L_{1s\text{-}C}$ value at the receiver. The next three columns are three different noise prediction methods: Industry Noise (Ind Støy), Nord2000Road (N2R) and the LF-model (LF07). The frequency interval for Ind Støy and N2R is 12,5-10 kHz, while for the LF07 method is 1-100 Hz. Results for the empirical prediction method (Finnskogen) are summarized in the next three columns.

We have also included a combination of the LF-method and N2R-method. We have run the LF-method from 1 Hz to 25 Hz and then N2R-method from 25 Hz to 10 kHz. The last column is the energy sum of these two methods. This is motivated by the possibility of introducing a new kernel that consists of the sum of the low frequency part from LF07 and the higher frequency part from N2R.

5.1 C2 - Short range propagation

C2 represents the measurements at Haslemoen in June 1994 and February 1995. A complete description of C2 can be found in [63, 61]. The topography and weather conditions are fairly easy for

modelling. The terrain is almost flat and the temperature gradient and wind speed are quite small. There are relatively short distances between the source and the receiver, 195-1407 meters. Ind Støy and N2R gives about the same predicted levels. It seems that MS slightly underpredicts the noise level this close to the weapon.

Summer measurements												
File	Dist	C4	Meas	Ind Støy	N2R	LF07	Finnskogen emp. mod.			LF07	N2R	LF+N2R
	[m]	[kg]				→100 Hz		-std	+std	→25 Hz	25 Hz→	Sum
15	195	1	120.2	116.5	117.7	106.8	115.4	106.1	124.7	106.8	117.4	117.7
16	259	1	116.9	114.4	115.2	103.8	111.4	102.1	120.7	103.8	114.9	115.2
17	431	1	111.4	110.3	110.6	98.0	109.3	100.1	118.6	98.0	110.3	110.5
20	1307	1	100.9	100.9	100.4	84.9	95.8	86.6	105.1	84.9	100.0	100.1
22	195	1	120.5	116.5	117.7	106.8	119.8	110.5	129	106.8	117.4	117.7
23	259	1	117.3	114.4	115.2	103.8	125.5	116.3	134.7	103.8	114.9	115.2
24	431	1	113.3	110.3	110.6	98.0	117.9	108.7	127.1	98.0	110.3	110.5
25	765	1	107.4	105.5	105.4	91.1	114.2	105.0	123.4	91.1	105.1	105.2
26	1109	1	103.1	102.2	101.9	87.1	105.6	96.4	114.8	87.1	101.6	101.7
27	1307	1	100.8	100.9	100.5	84.9	103.2	94.0	112.5	84.9	100.1	100.2
28	1406	1	99.6	100.3	99.8	84.3	102.1	92.8	111.3	84.3	99.4	99.5
29	195	1	120.5	116.5	117.7	106.8	120.0	110.8	129.2	106.8	117.4	117.7
30	259	1	117.7	114.4	115.2	103.8	115.8	106.6	125.0	103.8	114.9	115.2
31	431	1	111.7	110.3	110.6	98.0	108.3	99.1	117.6	98.0	110.3	110.5
32	765	1	106.2	105.5	105.4	91.1	101.1	91.8	110.4	91.1	105.1	105.2
33	1109	1	101.3	102.2	101.9	87.1	94.8	85.5	104.1	87.1	101.6	101.7
34	1307	1	100.5	100.9	100.4	84.9	93.5	84.2	102.8	84.9	100.1	100.2
35	1406	1	101.1	100.3	99.8	84.3	92.4	83.1	101.7	84.3	99.4	99.5
36	259	8	124.1	120.5	120.4	116.9	130.2	121.0	139.4	116.9	120.1	121.7
37	431	8	120.2	116.4	115.8	111.6	122.8	113.6	132.1	111.6	115.5	116.9
39	1109	8	109.6	108.4	107.1	101.8	109.8	100.6	119.1	101.8	106.7	107.9
40	1307	8	108.3	107.0	105.5	100.2	96.1	86.8	105.5	100.2	105.1	106.3
41	259	8	125.7	120.5	120.4	116.9	123.4	114.1	132.7	116.9	120.1	121.7
42	431	8	119.8	116.4	115.8	111.6	111.4	102.1	120.8	111.6	115.5	116.9
44	1109	8	111.0	108.4	107.0	101.8	98.4	89.1	107.7	101.8	106.7	107.9
45	1307	8	108.0	107.0	105.5	100.2	106.8	97.5	116.1	100.2	105.1	106.3

Table 5.1: Results for C2. All noise levels are in dB and equivalent to the MS level $L_{1s\text{-}C}$. Where nothing else is stated, the calculation is run from 12.5 Hz to 10 kHz.

5.2 C1 - Long range propagation

C1 is a more demanding test case, both due to more complex topography as well as the larger source-receiver distances, between 2 and 15.8 km. The weather conditions are also more demanding than in C2.

Generally Table 5.2 shows that Ind Støy and N2R gives roughly the same predictions. However, for

some cases N2R predict values that are very far from the measured values. This behaviour is hard to explain, but we observe that it typically occurs for propagation at long distances over hilly terrain.

We also see that Ind Støy generally seems to overpredict at large distances. As a "worst case" prediction tool, it seems reasonably accurate at medium distances, and a bit conservative at longer distances.

File no	Sensor	Dist	$cos\theta$	Meas	Ind Støy	N2R	LF07	Finnskogen			LF07	N2R	LF+N2R
		[km]					–100 Hz		-	+	–25 Hz	25 Hz–	Sum
70	306	2	-0.08	83.8	97.9	95.9	78.6	88.9	79.6	98.1	79.2	95.3	95.4
76	306	2	-0.12	87.8	97.9	95.9	78.6	88.9	79.6	98.1	79.2	95.3	95.4
136	306	2	0.32	89.9	97.9	98.4	78.6	97.8	88.6	107.0	79.2	97.7	97.7
144	306	2	-1	85.9	97.9	96.0	78.6	88.3	79.1	97.6	79.2	95.4	95.5
150	306	2	-0.96	72.0	97.9	95.5	78.6	88.1	78.9	97.4	79.2	94.9	95.0
168	306	2	0.93	100.1	97.9	102.8	78.6	91.5	82.3	100.7	79.2	102.2	102.2
174	306	2	0.72	97.2	97.9	103.6	78.6	90.4	81.2	99.7	79.2	103	103
180	306	2	-0.34	87.3	97.9	97.9	78.6	89.9	80.7	99.1	79.2	97.4	97.4
70	0	3.9	0.08	83.2	84.5	78.3	71.4	79.8	70.5	89.1	72.0	77.1	78.2
76	0	3.9	0.12	80.6	84.5	78.3	71.4	79.8	70.5	89.1	72.0	77.1	78.2
144	0	3.9	1.0	81.2	84.5	78.2	71.4	80.0	70.7	89.3	72.0	77.0	78.2
150	0	3.9	0.96	82.7	84.5	78.3	71.4	80.2	70.9	89.5	72.0	77.1	78.2
168	0	3.9	-0.93	83.6	84.5	82.4	71.4	81.2	72.0	90.4	72.0	81.8	82.2
174	0	3.9	-0.7	80.5	84.5	79.9	71.4	80.4	71.2	89.7	72.0	78.8	79.6
180	0	3.9	0.34	79.6	84.5	80.7	71.4	80.8	71.5	90.5	72.0	79.7	80.3
136	412	12	-0.52	75.7	77.1	57.9	57.4	62.7	53.5	72.0	57.4	56.8	60.1
168	412	12	-0.43	59.0	77.1	80.7	57.4	62.2	56.0	74.4	57.4	80.1	80.1
174	412	12	-0.37	58.1	77.1	80.8	57.4	64.2	55.0	73.5	57.4	80.2	80.2
180	412	12	-0.40	58.9	77.1	80.8	57.4	64.2	55.0	73.5	57.4	80.2	80.2
168	112	15.8	-0.82	71.1	80.0	63.8	53.7	62.2	53.0	71.4	54.4	63.2	63.7
174	112	15.8	-0.95	68.7	80.0	57.3	53.7	60.9	51.7	70.2	54.4	56.7	58.7
180	112	15.8	-0.95	57.2	80.0	60.1	53.7	61.2	51.9	70.4	54.4	59.5	60.6
168	212	12.5	-0.62	67.7	72.5	66.3	56.9	65.2	56.0	74.4	57.6	66.2	66.7
180	212	12.5	0.99	60.8	72.5 [1]	77.2	56.9	64.7	55.5	73.9	57.6	76.5	76.5

Table 5.2: Results for C1. All noise levels are in dB and equivalent to the MS level $L_{1s\text{-}C}$. Where nothing else is stated, the calculation is run from 12.5 Hz to 10 kHz. The source position number is 304.

5.3 M109 Hjerkinn

Noise measurements from M109 were made at Fokstugu 7 km from the weapon (Table 5.3). We predicted the noise from M109 at Fokstugu based on the new emission data in NMS. The results are presented in Table 5.4.

[1] This value was misprinted in [63].

shot	shot nr.	time	grenade	L_{CE} [dB]
140-2	-	10:27	OEF3 BB	90.3
141-1	1	10:47	RH662	94.3
141-2	2	10:53	RH663	98.2
142-1	6	11:25	DM662	90.1
142-2	7	11:32	DM662	91.4
142-3	8	11:49	DM662	91.0
142-4	9	11:54	DM662	88.3
142-5	10	12:00	DM662	92.6
142-6	11	12:06	DM662	94.6
142-7	12	12:17	DM662	87.8
142-8	13	12:22	DM662	88.5
143-1	14	12:47	DM662	96.1
143-2	15	12:54	DM662	89.2
143-3	16	13:01	DM662	97.6
144-1	3	13:51	RH662	91.6
144-2	4	13:57	RH662	93.2
143-4	-	14:12	DM662	88.5
143-5	17	14:19	DM662	99.5
143-6	18	14:24	DM662	92.5
143-7	19	14:35	DM662	91.2
143-8	20	14:44	DM662	87.7
133-1	21	15:02	DM662	88.5
144-3	5	16:10	RH662	89.1
133-2	22	16:19	DM662	95.7
133-3	23	16:24	DM662	88.9
133-4	24	16:31	DM662	92.6
133-5	-	16:37	DM662	94.0
133-6	-	16:42	DM662	87.8
133-7	-	16:47	DM662	87.0
133-8	25	17:02	DM662	91.4

Table 5.3: Measured noise level (C-weighted SEL) at Fokstugu, 7 km from the source.

The empirical model (Section 3.5) is only constructed for spherical detonations. There should, however, not be a problem to change NMS such that the empirical model can be applied for directive weapons. To apply the empirical model for the M109 data, we had to define the source as a blast of TNT in MS. We chose 8 kg TNT as an equivalent source for M109. This choice is based on the total energy released from a M109 muzzle in the direction of the sensor at 7 km. Calculation of the energy released from the M109 muzzle was done by the IBHVG2 code, and was confirmed by the measurements at 250 m.

Somewhat surprisingly we see from Table 5.4 that the measured sound level is underpredicted by about 10 dB. Given the large variation of noise levels under different conditions these measurements consisted of too few measurements to give a significant conclusion regarding this underprediction. Another possible cause of this underprediction may be the measurement trailer used for the mea-

surements at Fokstugu. Although we have no indications of a malfunction, we have not had the possibility to check the accuracy of this equipment.

For the computations for Hjerkinn (Table 5.4) we have applied new emission data for M109 [20]. This emission data set covers 1/3-octave band frequencies from 0.8 Hz and up to 20 kHz. Due to the limitations in NMS, the calculations include the frequencies between 0.8 Hz and 5 kHz. As most of the energy lie around 16 Hz, this limitation should not influence the predicted values. The older M109 emission data set in MS starts at 32 Hz in 1/1-octave frequency band. This may explain the low predicted values by LF07 method in table 5.4. The LF07 method is valid for the frequency range 1-100 Hz.

C-weighted predicted values at Fokstugu									
Source	Ind Støy	N2R	LF07	Finnskogen			LF07	N2R	LF+N2R
			–100 Hz		-	+	–25 Hz	25– Hz	SUM
M109-STD	88.0	88.5	30.9	82.2	72.9	91.4	7.5	87.8	87.8
M109-FFI-STD	90.8	89.8	79.6	82.2	72.9	91.4	79.6	89.3	89.7
M109-Fokstugu	85.4	86.9	25.1	82.2	72.9	91.4	6.4	86.1	86.1
M109-FFI-Fokstugu	88.4	88.2	79.3	82.2	72.9	91.4	79.3	87.6	88.1

Table 5.4: Predicted noise levels (C-weighted SEL) at Fokstugu, 7 km from the source. "M109" indicates that the old source has been used. "M109-FFI" indicates that the new source has been used. "STD" is the standard weather conditions in Milstøy. "Fokstugu" indicates that the weather conditions at the receiver has been used for the calculation. Where nothing else is stated, the calculation is run from 12.5 Hz to 10 kHz.

Unweighted predicted values at Fokstugu			
Source	LF07	LF07	N2R
	1-100 Hz	1-25 Hz	25-10 kHz
M109-Lin	42.1	11.9	90.7
M109-FFI-Lin	98.2	98.2	92.1

Table 5.5: Predicted noise levels (Unweighted SEL) at Fokstugu, 7 km from the source.

In Figure 5.1 we see the amount of the energy from a shot with M109 that is below or above 25 Hz. There is about 8 dB more (C-weighted) energy above 25 Hz. This is relevant when we consider results for the three last columns in Figures 5.1, 5.2 and 5.4. As we see, for the C-weighted SEL of the M109, the contribution from LF07 is very small. However, this would not be the case for large detonations. We see in the tables that the relationship between LF07 and N2R seems reasonable in relation to the source in Figure 5.1.

From Table 5.5 we see that the old source data for M109 (starting at 32 Hz) should not be used for the new LF-model.

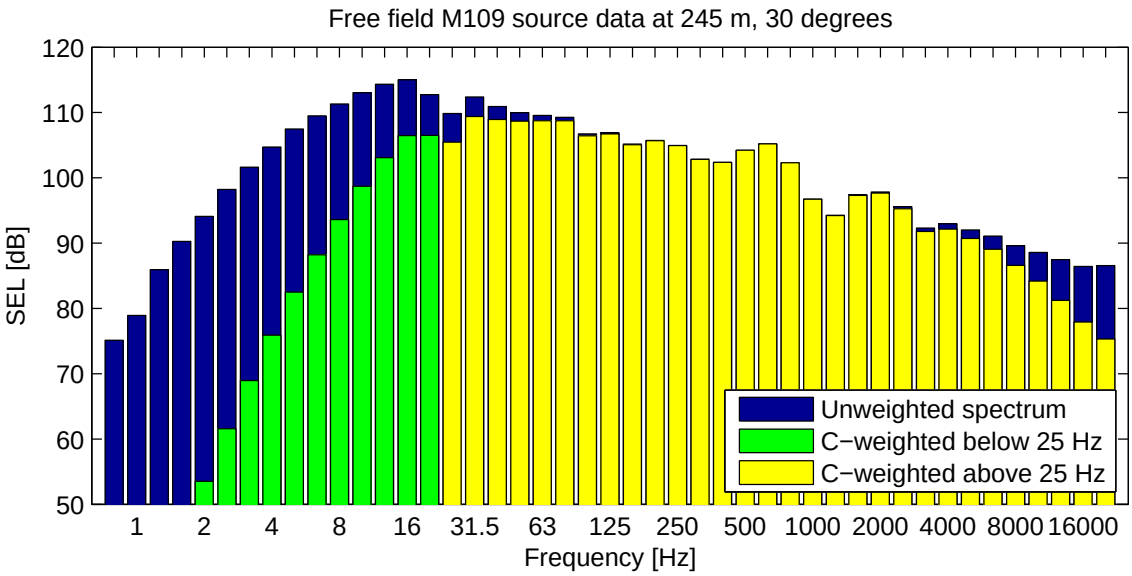

Figure 5.1: The weighted total energy level is $L_{CE} = 119.4$ dB. Below 25 Hz (green) the total energy level is $L_{CE} = 110.8$ dB. Above 25 Hz (yellow) the sum energy is $L_{CE} = 118.8$ dB.

5.4 Summary of test results

Typical use of MS (for large weapons) is for distances of up to 7 km and L_{CE} above 100 dB. The long range test (12–15 km) considered may not be relevant, because the measured levels are much lower than 100 dB. However, it still reveals interesting aspects about MS.

We have tested all prediction models available in NMS in three cases. We see that the prediction methods Industry Noise and N2000road give results quite close to each other, for distances up to 7 km. The predicted values are close to the measurements in the case with flat terrain, short source-receiver distances (up to 1400 m), and almost neutral weather conditions.

For the low level (57-76 dB) long range propagation (12–15 km) there are larger differences between the measurements and the predicted values. These differences seem to be partly random. N2R appear to have some unresolved stability issues in such demanding situations.

The calculations for M109 at 7 km show an underprediction of about 10 dB. Ind Støy and N2R produce similar results.

The number of test cases considered in this section is far too few to be significant in evaluating the performance of NMS. More and extensive testing will be required to validate NMS before it can be used for production of noise maps.

6 Conclusions

This report summarizes the work that has been done to increase the ability of NODEA to calculate the noise level near military installations. During the project period 30 reports, 9 conference proceedings and one journal paper have been published, shedding considerable light on the different aspects of this broad range of topics. This should serve as a good documentation of the improved methods and as a basis for further work on this problem.

Emission data for several old and new weapons have been included in the emission database of NMS. This increases the accuracy of the calculated noise maps for these weapons.

New computational kernels have been included in NMS. At this point it has not been possible to sufficiently validate these new kernels against measurements. While NMS seems promising, it still needs development and validation before it may be used in practice.

Insulation of houses from low frequency noise and vibration has been considered. Suggestions have been provided for constructing better residential buildings, however no satisfactory method of modifying existing homes has yet been found. New methods for evaluation of indoor low frequency noise have also been suggested.

References

[1] M. Huseby, R. Rahimi, J. A. Teland, and I. Dyrdal. Støy fra skytefelt. FFI/RAPPORT - 2005/00471, Norwegian Defence Research Establishment, 2005.

[2] W. Weber. Das schallspektrum von knallfunken und knallpistolen mit einem beitrag über die anwendungsmöglichkeiten in der elektroakustischen meßtechnik. *Akustische Zeitschrift*, 4:373–391, 1939.

[3] K. W. Hirsch. On the influence of local ground reflections on sound levels from distant blasts at large distances. *Noise Control Eng. J.*, 46(5):215–226, 1998.

[4] ISO/DIS 17201-2. Acoustics – noise from shooting ranges – part 2: Estimation of source data for muzzle blast and projectile noise, 2004.

[5] M. Huseby and H. P. Langtangen. A finite element model for propagation of noise from weapons over realistic terrain. In *Proceedings Internoise 2006*, pages 1–8, paper 513, Honolulu, Hawaii, USA, 3–6 December, 2006.

[6] R. D. Anderson and K. D. Fickie. *IBHVG2 A User's guide*. Ballistic Research Laboratory, Aberdeen, USA.

[7] *AUTODYN Theory manual*. Century Dynamics Ltd.

[8] R. Rahimi, M. Huseby, and H Fykse. Ammunisjons og våpendata for bruk til beregning av støy fra skytefelt. FFI-notat 2006/01658 (konfidensielt), Norwegian Defence Research Establishment, 2007.

[9] J. A. Teland, R. Rahimi, and M. Huseby. Numerical simulation of sound emission from weapons. *Noise Control Eng. J.*, 55(4), 2007.

[10] M. Huseby, R. Rahimi, J. A. Teland, and C. E. Wasberg. En sammenligning av beregnet og målt lydtrykk nær lette våpen. FFI/RAPPORT - 2006/00261, Norwegian Defence Research Establishment, 2006.

[11] B. L. Madsen, J. Andersen, and E. A. Andersen. Dokumentasjon av beregningsprogrammet FOFTlyd version 0.4. Technical Report FOFT M-45/1997, Forsvarets Forskningstjeneste, Danmark, 1997.

[12] W. E. Baker. *Explosions in air*. Austin, University of Texas Press, first edition, 1973. ISBN 0–292–72003–3.

[13] J. W. Reed. Atmospheric attenuation of explosion waves. *J. Acoust. Soc. Am.*, 61(1):39–47, 1977.

[14] M. Huseby, I. Dyrdal, H. Fykse, and B. Hugsted. Målinger av lydtrykket i nærfeltet til en rifle. FFI/RAPPORT - 2005/03998, Norwegian Defence Research Establishment, 2005.

[15] M. Huseby, B. Hugsted, I. Dyrdal, H. Fykse, and A. Jordet. Målinger av lydtrykket nær lette våpen, Terningmoen, revidert utgave. FFI/RAPPORT - 2006/00260, Norwegian Defence Research Establishment, 2006.

[16] M. Huseby, B. Hugsted, and A. C. Wiencke. Målinger av lydtrykket nær CV90, AGL og 12.7, Rena. FFI-rapport 2006/01657, Norwegian Defence Research Establishment, 2007.

[17] M. Huseby, R. Rahimi, and J. A. Teland. Noise from firing ranges. In R. Korneliussen, editor, *Proceedings 29th Scandinavian Symposium on Physical Acoustics*, Ustaoset, Norway, 29 Jan–1 Feb, 2006. ISBN 82-8123-001-0.

[18] J. A. Teland, R. Rahimi, and M. Huseby. Numerical simulation of sound emission from weapons. In *Proceedings Internoise 2006*, pages 1–10, paper 526, Honolulu, Hawaii, USA, 3–6 December, 2006.

[19] S. Å. Storeheier. Eksempler på bestemmelse av sel-spektra for akustiske trykkpuls tidshistorier. Notat 90-NO060011, SINTEF, 2006.

[20] M. Huseby. Noise emission data for M109, 155 mm field howitzer. FFI-rapport 2007/02530, Norwegian Defence Research Establishment, 2007.

[21] S. Å. Storeheier and K. Selvåg. Bestemmelse av akustisk impedans og frittfeltskorreksjon på standplass for emisjonsmåling av lette våpen, Terningmoen. Notat 90-NO050203, SINTEF, 2006.

[22] M. Huseby. Emisjonsdata for støy fra CV90 (30 mm) og NM218 (12.7 mm). FFI-rapport 2007/02633, Norwegian Defence Research Establishment, 2007.

[23] M. Huseby, K. O. Hauge, E. Andreassen, and N. I. Nilsen. Målinger av lydtrykket nær M109, 155 mm felthaubits. FFI-rapport 2006/01657, Norwegian Defence Research Establishment, 2007.

[24] Ra Cleave. Near field acousto-seismic response due to heavy artillery shooting. Technical Report 20071037-7, Norwegian Geotechnical Institute, December 2007.

[25] ISO 9613-2. Acoustics – attenuation of sound during propagation outdoors – part 2: General method of calculation, 1996.

[26] B. Plovsing and J. Kragh. Nord2000. Comprehensive outdoor sound propagation model. Part 1: Propagation in an atmosphere without significant refraction. DELTA Acoustica & vibration report AV 1849/00, 2001.

[27] B. Plovsing and J. Kragh. Nord2000. Comprehensive outdoor sound propagation model. Part 1: Propagation in an atmosphere with refraction. DELTA Acoustica & vibration report AV 1851/00, 2001.

[28] H. Olsen. Forsvarsbygg FoU-prosjekt 2007, implementering av nye LF-algoritmer i milstøy, oppsummering. Notat 90E242/ho, SINTEF, 2008.

[29] G. Taraldsen. Notes on the ground effect for low frequency noise. SINTEF MEMO 90E242, 2008.

[30] M.E. Delany and E.N. Bazley. Acoustical properties of fibrous absorbent materials. *Appl.Acoust.*, 3:105–116, 1970.

[31] G. Taraldsen. The Delany-Bazley impedance model and Darcy's law. *Acta acustica*, 91:41–50, 2005.

[32] K. Attenborough, K.M. Li, and K. Horoshenkov. *Predicting outdoor sound*. Taylor and Francis, 2007.

[33] A.D. Pierce. *ACOUSTICS. An introduction to its physical principles and applications*. Acoustical Society of America, 1994.

[34] M. Abramowitz and I.A. Stegun, editors. *Handbook of mathematical functions with Formulas, Graphs, and Mathematical Tables*. Dover (ninth printing), 1972.

[35] G. Taraldsen. Ground effect for low frequency waves. 30^{th} *Scandinavian symposium on physical acoustics*, 2007.

[36] G. Taraldsen. Unbounded ground effect in outdoor noise propagation. 31^{th} *Scandinavian symposium on physical acoustics*, 2008.

[37] G. Taraldsen. A note on reflection of spherical waves. *J. Acoust. Soc. Am.*, 117:3389–3392, 2005.

[38] J-F Allard et al. Impedance measurements around grazing incidence for nonlocally reacting thin porous layers. *J. Acoust. Soc. Am.*, 113:1210–1215, 2003.

[39] J. F. Allard, M. Henry, V. Gareton, G. Jansens, and W. Lauriks. Impedance measurements around grazing incidence for nonlocally reacting thin porous layers. *J. Acoust. Soc. Am.*, 113(3):1210–1215, 2003.

[40] C.J. Hickey et al. Impedance and Brewster angle measurement for thick porous layers. *J. Acoust. Soc. Am.*, 118:1503–1509, 2005.

[41] J. F. Allard and M. Henry. Fluid-fluid interface and equivalent impedance plane. *Wave Motion*, 43(3):232–240, 2006.

[42] K. M. Li, T. Waters-Fuller, and K. Attenborough. Sound propagation from a point source over extended-reaction ground. *Journal of the Acoustical Society of America*, 104(2):679–685, 1998.

[43] Finn Løvholt. Ground classification. Technical Report 20071037-5, Norwegian Geotechnical Institute, December 2007.

[44] Eyvind Aker. NORTRIAL databasen. Technical Report 20061034-2, Norwegian Geotechnical Institute, April 2007.

[45] Eyvind Aker. The NORTRIAL database. Technical Report 20061034-3, Norwegian Geotechnical Institute, April 2006.

[46] Karin Rothschild. NORTRIAL - Innlegging av måledata fra Rødsmoen og Lista. Technical Report 20071037-2, Norwegian Geotechnical Institute, March 2007.

[47] Eyvind Aker. NORTRIAL - Innlegging av måledata fra Finnskogen 1994 og 1996. Technical Report 20071037-3, Norwegian Geotechnical Institute, April 2007.

[48] Eyvind Aker. NORTRIAL - Adding measured data from Finnskogen 1994 and 1996. Technical Report 20071037-4, Norwegian Geotechnical Institute, April 2007.

[49] Karin Rothschild. NORTRIAL - Innlegging av måledata fra Haslemoen. Technical Report 20071037-1, Norwegian Geotechnical Institute, February 2007.

[50] C. M. Madshus, E. Aker, F. Løvholt, R. Cleave, and N. I. Nilsen. NORTRIAL database on long range low frequency sound and vibration propagation. INTER-NOISE 2006, December 2006.

[51] C. M. Madshus, E. Aker, R. Cleave, H. R. Cederkvist, N. I. Nilsen, and S. Å. Storeheier. Use of statistical methods in the development of empirical prediction models for long range low frequency sound and vibration propagation. INTER-NOISE 2006, December 2006.

[52] Finn Løvholt and Zenon Medina-Cetina. Statistical modelling of sound propagation. Technical Report 20071037-6, Norwegian Geotechnical Institute, December 2007.

[53] M. Huseby and H. P. Langtangen. Modeling propagation of noise over three-dimensional terrains. In B. Skallerud and H. I. Andersson, editors, *Proceedings MekIT'03 Computational Mechanics*, pages 175–188, Trondheim, Norway, 8–9 May, 2003. ISBN 82-519-1868-5.

[54] M. A. Biot. Mechanics of deformation and acoustic propagation in porous media. *J. Appl. Phys.*, 33(4):1482–1498, 1962.

[55] M. Huseby, H. P. Langtangen, and D. E. Reksten. A three-dimensional model for noise propagation over realistic terrain. In U. Kristiansen, editor, *Proceedings 27th Scandinavian Symposium on Physical Acoustics*, Ustaoset, Norway, 25–28 Jan, 2004. ISBN 82-8123-000-2.

[56] M. Huseby. A finite element model for noise from firing ranges. In *Proceedings Internoise 2005*, pages 1–10, paper 1831, Rio de Janeiro, Brazil, 7–10 August, 2005.

[57] Z. E. A. Fellah and C. Depollier. Transient acoustic wave propagation in rigid porous media: A time-domain approach. *J. Acoust. Soc. Am.*, 107(2):683–688, 2000.

[58] Z. E. A. Fellah and C. Depollier. On the propagation of acoustic pulses in porous rigid media: A time-domain approach. *J. Comp. Acoust.*, 9(3):1163–1173, 2001.

[59] B. L. Andersson, A. Cederholm, M. Huseby, I. Karasalo, and U. Tengzelius. Validation of a ray-tracer for long range noise-prediction using noise measurements from Finnskogen available in the NORTRIAL database. In R. Korneliussen, editor, *Proceedings 30th Scandinavian Symposium on Physical Acoustics*, Ustaoset, Norway, 28–31 Jan, 2007. ISBN 978-82-8123-002-6.

[60] A. Cederholm. Swedish Defence Research Agency (FOI), private correspondence, January 2008.

[61] R. Rahimi and M. Huseby. Innledende testing av utviklingsversjon av MILSTØY II: Testutvalg C2 fra NORTRIAL. FFI-notat 2007/01867, Norwegian Defence Research Establishment, 2007.

[62] M. Huseby. A selection of data from measurements of C4 detonations at Finnskogen in 1994, test case C1. FFI-rapport 2007/00528, Norwegian Defence Research Establishment, 2007.

[63] R. Rahimi and M. Huseby. Innledende testing av utviklingsversjon av MILSTØY II: Testutvalg C1 fra NORTRIAL. FFI-notat 2007/00766, Norwegian Defence Research Establishment, 2007.

[64] H. Olsen. Forsvarsbygg FoU-prosjekt 2005–2007, Ubetjent måling av lyd og vibrasjoner på Rødmoen. Notat 90E292/ho, SINTEF, 2008.

[65] S. Å. Storeheier. Oppfølgning av "feltlab" for måling av støy fra sprengninger og tunge våpen. Oppsummering fra møte i rena leir 14 juni 2006. Notat 90-NO060109, SINTEF, 2006.

[66] Karin Rothschild. Analysis of measurements data from the Rødsmoen tests in december 2005. Technical Report 20071357-1, Norwegian Geotechnical Institute, January 2008.

[67] T. Gjestland. Low frequency sound insulation in buildings. Report A210, SINTEF, 2006.

[68] G. Taraldsen. Measures against exterior low frequency sound and vibration impact on buildings. SINTEF MEMO 90E281, 2007.

[69] A. Pietrzyk. Sound insulation at low frequencies. *Doctoral thesis for the degree of Doctor of Philosophy, Chalmers University of Technology*, 1997.

[70] S. Pedersen, H. Møller, and K. Persson-Waye. Indoor measurements of low-frequency noise for annoyance assesment. *19th INTERNATIONAL CONGRESS ON ACOUSTICS MADRID*, 2007.

[71] K.K. Hodgdon, A.A. Atchley, and R.J. Bernhard. Low frequency noise study. *Partnership for AiR Transportation Noise and Emissions Reduction. An FAA/NASA/Transport Canada sponsored Center of Excellence report.*, 2007.